의학석사 학위논문

Amorphous Silica Nanoparticles Inhibit Gap Junctional Intercellular Communication via Mitogen-Activated Protein Kinase Pathway

무정형 실리카 나노물질의

Gap junction의 세포간 신호전달 억제 기전에 대한 연구

2019 년 8 월

서울대학교 대학원

의학과 중개의학 전공

이 광 훈

Amorphous Silica Nanoparticles Inhibit Gap Junctional Intercellular Communication via Mitogen-Activated Protein Kinase Pathway

지도교수 강 병 철

이 논문을 의학석사 학위논문으로 제출함

2019 년 4 월

서울대학교 대학원

의학과 중개의학전공

이 광 훈

이광훈의 석사 학위논문을 인준함

2019 년 7 월

위 원 장 _____ (인)

부 위 원 장 _____ (인)

위 원 _____ (인)

ABSTRACT

Amorphous Silica Nanoparticles Inhibit Gap Junctional Intercellular Communication via Mitogen-Activated Protein Kinase Pathway

Lee Gwang Hoon, D.V.M.

Graduate School of Translational Medicine, Department of Medicine

Seoul National University

Amorphous silica nanoparticles (SiNPs) are widely applied in various industries. Due to their relatively safe properties in comparison with crystalline silica nanoparticles, SiNPs have been used in medical field (such as targeted drug/DNA delivery, cancer therapy, enzyme immobilization, and dentistry as an abrasive agent) as well as food industry, cosmetics, and automotive industry. However, nanoparticles should be used with caution because of their unique physical and chemical characteristics. Some studies have revealed that SiNPs possess toxicity in recent years. Data on their potential toxicities are insufficient. Thus, the objective of this study was to focus on effects of SiNPs to gap junctional intercellular

communication (GJIC) in WB-F344 rat liver epithelial cells. For characterization, SiNPs was measured by ransmission electron microscopy (TEM) and dynamic light scattering (DLS). Particle diameter of SiNPs measured by TEM was 62.79 ± 11.26 and hydrodynamic size of SiNPs measured by DLS was 69.35 nm. For GJIC experiment, the highest concentration that showed no significant cytotoxicity was determined to be 5,000μg/ml in cytotoxicity test. SiNPs inhibited dye transfer the most (by 37.75%) at 12 hours after treatment compared to negative control in time course study of scrape/loading dye transfer. Furthermore, SiNPs inhibited GJIC in a dose-dependent manner based on results of scrape/loading dye transfer, immunofluorescence staining, and western blot analysis. SiNPs phosphorylated ERK1/2 and MEK kinases, but not PKC kinases, in a dose-dependent manner. Inhibition of GJIC induced by SiNPs was significantly recovered by ERK1/2 inhibitor and MEK inhibitor, but not by PKC inhibitor. Taken together, these results suggest that SiNPs can activate a hierarchical kinase program of MAPK signaling and induce inhibition of GJIC in WB-F344 rat liver epithelial cells. SiNPs are currently applied in clinical use, so appropriate dose should be used clinically, referring to this study, in which relatively high concentrations of SiNPs inhibited GJIC.

Keywords: Nanoparticles; silica; gap junctional intercellular communication; Cx43

Student number: 2014-21159

CONTENTS

LIST OF FIGURES

LIST OF ABBREVIATIONS

GJIC	gap junctional intercellular communication
SL/DT	scrape loading and dye transfer
Cx43	connexin 43
MAPKs	mitogen-activated protein kinases
PKC	protein kinase C
BIM I	bisindolymaleimide I
TPA	12-O-tetradecanocylphorbol-13-acetate

INTRODUCTION

Nanoparticles are substances that have at least one dimension below 100 nm. Due to their unique physical and chemical properties in comparison with their micro-sized or bulk counterparts, nanotechnology has become a significant technology in various fields such as electronics, chemistry, physics, and medicine in recent years. With fast-growing market of nanotechnologies, nanoparticles are very close to our everyday life. Benefits from nanotechnologies will produce sustainable development and new job, reaching a market of $3 trillion and creating 6 million jobs with essential societal needs and mass application by 2020 [1-5]. Silicon is one of the most abundant soil minerals on the earth. Silica dioxide is its oxide form and major constituents of sand and quartz contributing to 90% of the earth's crust [6]. This suggests that many people might have been exposed to silica dioxide. The Organization of Economical Cooperation and Development (OECD) Working Party on Manufactured nanomaterials has developed a strategic research plan on toxicology for nanoparticles. Silica dioxide dioxide was chosen as one of the OECD's priority list of representative manufactured nanomaterials for testing.

Silicon based materials are important for industrial products such as building, construction, cosmetics, adhesive, electronics, and food industry [6, 7]. Silicon can exist in three forms: crystalline silica, amorphous silica, and fused silica. It is well known that diseases related to silica such as silicosis and lung cancer are only associated with crystalline silica [8]. Contrary to crystalline silica, amorphous silica has been used in medical field (such as targeted drug/DNA delivery, cancer therapy,

enzyme immobilization, and dentistry as an abrasive agent), automotive industry, food industry, and cosmetics due to its relatively safe properties [1, 4, 9, 10]. For example, with encapsulation of enzymes, amorphous silica nanoparticle can prolong shelf life of bacteria and cells without changing their metabolic activities [6].

However, some recent studies have revealed that amorphous silica nanoparticles have toxicities, although some studies have shown that amorphous silica nanoparticles do not have toxicity. Wiemann et al. have studied pulmonary toxicity of amorphous silica both *in vitro* and *in vivo* [11]. Dose dependent release of LDH, GLU, TNF-α, and H_2O_2 *in vitro*, increased neutrophil in blood, and increased lymphocytes, polymorphonuclear neutrophils, atypical cells, and eosinophils in bronchoalveolar lavage fluid were found after exposure to amorphous silica [11]. Ahamed [10] has found that amorphous silica nanoparticle have cytotoxicity, causing oxidative stress and apoptosis of human skin epithelial cells and human lung epithelial cells. In contrast, Farcal et al. [4] have shown that amorphous silica nanoparticles do not induce cytotoxicity, cell transformation, or genotoxicity in mouse fibroblast cells. Ryu et al. [12] did not find any toxicity or change in organs after skin had contact with amorphous silica nanoparticle.

Due to unique physical properties of nanoparticles such as small size, large surface area, and surface reactivity that are different from those of microparticles or bulk, health effects of nanoparticles have received a lot of attention [13, 14]. Recently, adverse effects of nanoparticles have been reported from numerous studies. For example, Hackenberg et al. [15] have found that zinc oxide nanoparticles have cytotoxicity, genotoxicity, and inflammatory potential in nasal mucosa cells. Magaye et al. [16] have presented data showing that cobalt, nickel, and copper based

nanoparticles have genotoxicity and carcinogenicity. Warheit et al. [17] have found that nanoscale TiO_2 rods and nanoscale TiO_2 dots can induce transient inflammatory cells after pulmonary instillation in rats.

Gap junctional intercellular communication (GJIC) is composed of gap channel-forming integral membranes known as connexon, composed of six connexins with molecular mass of 26 to 56 kDa, that directly link cytoplasms of neighboring cells and allow passage of ions and signaling molecules, nucleotides, inositol triphosphate, Ca2+, second messengers, and other molecules less than 1kD in size that are essential cellular components for maintaining homeostasis, cell growth, proliferation, differentiation, tissue homeostasis and so on [24, 25].

Dysfunctional GJIC has recently been associated with lots of disease such as neuropathy [26], hereditary deafness [27], cataract [28], skin disease [29] and heart disease [30]. In addition to, as is widely known, dysfunctional GJIC is strongly linked to carcinogenesis because GJIC control cell growth [30, 31]. Most tumor cells have dysfunctional GJIC [32] and numerous reports have revealed the data that treatment of cells with tumor promoters can lead to decrease in gap junctional communication [30]. For example, Carcinogens such as DDT, 12-0-tetradecanoylphorbol-13-acetate, dieldrin and heptachlor epoxide inhibited GJIC [33-35]. In addition to, oncogene transfection induced inhibition of GJIC [36] and unknown substances such as ascorbic acid 6-palmitate and 18α-glycyrrherinic acid are tested by studying GJIC [37, 38].

Among connexin, Cx43 is major protein of connexin and phosphorylation of Cx43 is important to evaluate functional gap junctions [38]. Because WB-F344 rat liver

epithelial cells are stem-like cells and inherently express abundant connexin43, unlike most other cell lines, this cell line was chosen in the present study [39].

Nanoparticles can inhibit cells through a few routes. First, nanoparticles can affect various messenger proteins to trigger biological effect. Chang et al. [18] have found that Pep-1-coated quantum dots can inhibit GJIC by ERK dependent phosphorylation of Cx43. Chen et al. [19] have demonstrated that iron nanoparticle can inhibit osteogenic differentiation and affect signaling mechanism of β-catenin, a cancer/testis antigen, SSX, and matrix metalloproteinase 2 (MMP2) in human mesenchymal stem cells. Second, nanoparticles can pass through the cell membrane and into the nucleus to inhibit mRNA level, thus inhibiting the expression of protein. Tao et al. [20] have found silica nanomaterials in nuclei and cytoplasm by TEM. Arnoldussen et al. [21] have shown that carbon nanotubes can inhibit expression of Gjb1, one of connexin, at mRNA level. Third, nanoparticles can arouse reactive oxygen species known to have adverse effects on cells. Raghunathan et al. [22] have reported that chrome nanoparticle has genotoxicity by inducing reactive oxygen species. Kim et al. [23] have found that silver nanoparticles have toxicities by causing oxidative stress in human hepatoma cells. Furthermore, numerous studies have revealed toxicity and carcinogenicity of nanoparticles with their mechanisms. For example, zinc oxide nanoparticles have cytotoxicity, genotoxicity, and proinflammatory potential to human nasal mucosa cells examined by MTT test and single cell microgel electrophoresis (comet) assay. Titanium nanoparticles have respiratory toxicology. Cobalt-, nickel-, and copper-based nanoparticle have genotoxicity and carcinogenicity [15-17].

Lots of studies have been conducted on the toxicities of SiNPs, however, there has been no study about effect to GJIC of SiNPs. Accordingly, the aim of this study was to investigate cytotoxicity and effect to GJIC of SiNPs and determine the underlying related molecular mechanisms of gap junctional inhibition in WB-F344 rat liver epithelial cells.

MATERIALS AND METHODS

Chemical and reagents

SiNPs (Declared particle size: 15-20nm) was purchased from Nanostructured & Amorphous Materials Inc (Houston, TX, USA). Stock suspensions of particles were prepared in ddH_2O by sonication for 1hour (pulse on 30s/off 30s by one cycle) in dark room for preventing the effect of light before all experiments. Bovine serum albumin was purchased from Amresco (Solon, OH, USA). Lucifer yellow CH dilithium salt powder, dimethlsulfoxide(DMSO), 12-O-tetradecanocylphorbol-13-acetate (TPA), The ERK inhibitor PD98059 and MEK inhibitor U0126 were purchased from Sigma-aldrich. PKC inhibitor bisindlymaleimide I (BIM I) was purchased from Calbiochem (San Diego, CA, USA).

Physic-chemical characterization

Particle size and morphology of SiNPs and silica micro particle (SiMPs) was evaluated with a transmission electron microscope (TEM, JEOL 2010f instrument). This suspension in water was pipetted onto formvar/carbon-coated TEM grid. After droplets were left to dry at room temperature, they were photographed. Sizes of 20 particles on the grid were measured and their average value was calculated. Hydrodynamic size and zeta potential of SiNPs and SiMPs were determined by Dynamic Light Scattering (DLS) with a Zetasizer Nano-ZS instrument. After the

stock solution was sonicated and diluted to concentration of 0.1 mg/ml recommended by the manufacturer, sizes were measured.

Cytotoxicity assay

Cytotoxicity was measured by trypan blue exclusion assay as described by Strober [40] with some modifications. In brief, WB-F344 cells were seeded onto a 24-well plate and grown in D-medium (Gibco, Carlsbad, CA, USA) supplemented with 5% FBS (Gibco), 0.5% PSN antibiotic mixture (Gibco), sodium bicarbonate (Amresco, Solon, OH, USA), sodium pyruvate (Sigma-Aldrich), d-glucose (Sigma-Aldrich), and sodium chloride (Sigma-Aldrich) at 37℃ in a 5% CO2 humidified incubator. To determine the concentration that would result in 70~80% viability compared to negative control, WB-F344 cells were exposed to SiNPs at different concentrations (0-5,000 μg/ml) for 24 hours. Stained and unstained cells were counted after a mixture of 0.4% trypan blue and cell suspension was incubated at room temperature for 3 minutes before applying to a hemocytometer. Viability was determined as the percentage of cells with clear cytoplasm (viable cells) versus cells that contained trypan blue in the cytoplasm (dead cells). All experiments were performed in triplicate.

Scrape-Loading/Dye Transfer assay for GJIC

Scrape-Loading/Dye Transfer (SL/DT) assay was used to measure GJIC using published method [35]. In brief, for time-dependent inhibition study of GJIC, WB-

F344 cells were incubated with 5,000 μg/ml SiNPs suspension as optimal dose determined by cytotoxicity test for up to 24 hours. For dose-dependent inhibition study of GJIC, cells were incubated with 5,000 μg/ml, 1,000 μg/ml, and 200 μg/ml of SiNPs for 24 hours. After cells were washed 3 times with D-PBS (PBS without Ca2+ and Mg2+), 0.05% lucifer yellow in D-PBS was added to cells and six scrapes were made with a surgical steel surgical blade. After 9 minutes of incubation at room temperature, lucifer yellow was discarded. Cells were washed 3 times with D-PBS and fixed with 4% formaldehyde solution in D-PBS.

Immunofluorescence staining of Cx43

Immunofluorescence staining was carried out to verity the quantification and localization of Cx43 protein expression. WB-F344 cells were seeded onto the 8 well chamber slide and treated with same concentration as dose-dependent SL/DT assay of SiNPs. WB-F344 cells were blocked with 3% bovine serum albumin in PBS containing 0.05% Tween 20 for 1 hour at room temperature. After supernatant was discarded, cells were incubated overnight at in 1:1500 rabbit polyclonal anti-Cx43 antibody **(**Sigma-Aldrich, St. Louis, MO, USA) in PBS with 1% BSA at 4℃ for overnight. After washed 3 times, The cells were incubated with 1:800 goat anti rabbit IgG Alexa fluor 488 secondary antibody (Molecular Probes, Eugene, OR, USA) in PBS with 1% BSA for 1 hour at room temperature. Cells were washed 3 times with D-PBS and fixed with 4% paraformaldehyde for 20 minutes at room temperature. Cells were observed and photographed with inverted microscope and quantified by

counting the number of communicating cells to judge the activity of the gap junction channel. Samples were mounted in vectashield with DAPI (Vector Laboratory, Burlingame, CA, USA) and photographed on inverted fluorescent microscope.

Western blot analysis of Cx43

Western blot analysis was used to measure the phosphorylation state of Cx43, ERK, MEK and PKC. After WB-F344 cells was treated with same concentration as dose-dependent SL/DT assay and immunofluorescence of SiNPs, proteins were extracted by RIPA buffer (Millipore, Bedford, MA, USA) containing 0.1% protease inhibitor cocktail (Sigma-Aldrich) and phosphatase inhibitor cocktail 2 (Sigma-Aldrich), phosphatase inhibitor cocktail 3 (Sigma-Aldrich) and centrifuged at 13,000rpm for 20 minutes at 4℃. The protein contents were determined using BCA protein assay kit (Pierce Biotechnology, Rockford, IL, USA) and 20μg proteins determined from each sample were mixed with 2X Laemmli sample buffer and separated on 12% SDS-polyacrylamide gel at 80v for 20min and then 110v for 3 hours and transferred to polyvinylidene difluoride membranes (Bio-Rad, Richmond, CA, USA) at 100V for 1 hour. Membrane was blocked with 5% skim milk in Tris-buffered saline (TBST) solution for 1 hour to reduce non-specific binding. After membrane was washed three times for 15 minutes respectively with TBST, membranes was incubated with anti-Cx43 (1:3000, Sigma-Aldrich) in 3% BSA, anti-pERK1/2 (1:2000, Cell signaling Technology, Beverly, MA, USA), anti-ERK1/2 antibodies (1:2000, Cell signaling Technology), anti-pMEK inhibitors (1:2000, Cell signaling Technology), anti-MEK inhibitors (1:1000, Cell signaling Technology),

anti-PKC inhibitors (1:1000, Santa Cruz Biotechnology, CA, USA) or anti-pPKC inhibitors (1:1000, Biovison Incoporated, CA, USA) in 5% BSA in TBST for overnight at 4℃. After washing 3 times, membrane was incubated with secondary antibody conjugated to horseradish peroxidase for 2 hours at room temperature. ECL kit was used to provide chemiluminescence and the western blot analysis including relative band intensity and phosphorylation state was quantified by an image-analysis program using Image J (Bethedsa, MD, USA) or Scion Image (NIH, Bethesda, MD, USA) [41].

Recovery effect of inhibitors on the inhibition of GJIC

For study on recovery effect of inhibitors on the inhibition of GJIC, WB-F344 cells were pretreated with 50μM ERK PD98059, 10μM of MEK inhibitor U0126, and 10μM PKC inhibitor BIM I for 30 minutes before exposure to SiNPs.

Statistical analysis

The data were expressed as means ± SD. Statistical analysis was performed using a one-way ANOVA or Student's t-test using SPSS software version 24 (SPSS Inc., Chicago, IL, USA). P values$\leq$0.05 were considered statistically significant.

Results

Particle characterization of SiNPs

The measured TEM-size of SiNPs was 62.79 ± 11.27nm and 357.20 ± 76.30nm (Fig. 1). DLS-analysis showed a hydrodynamic size of SiNPs with 70.34 nm. The zeta potential of SiNPs in water diluted to 0.1mg/ml was -32.2mV (Fig. 2).

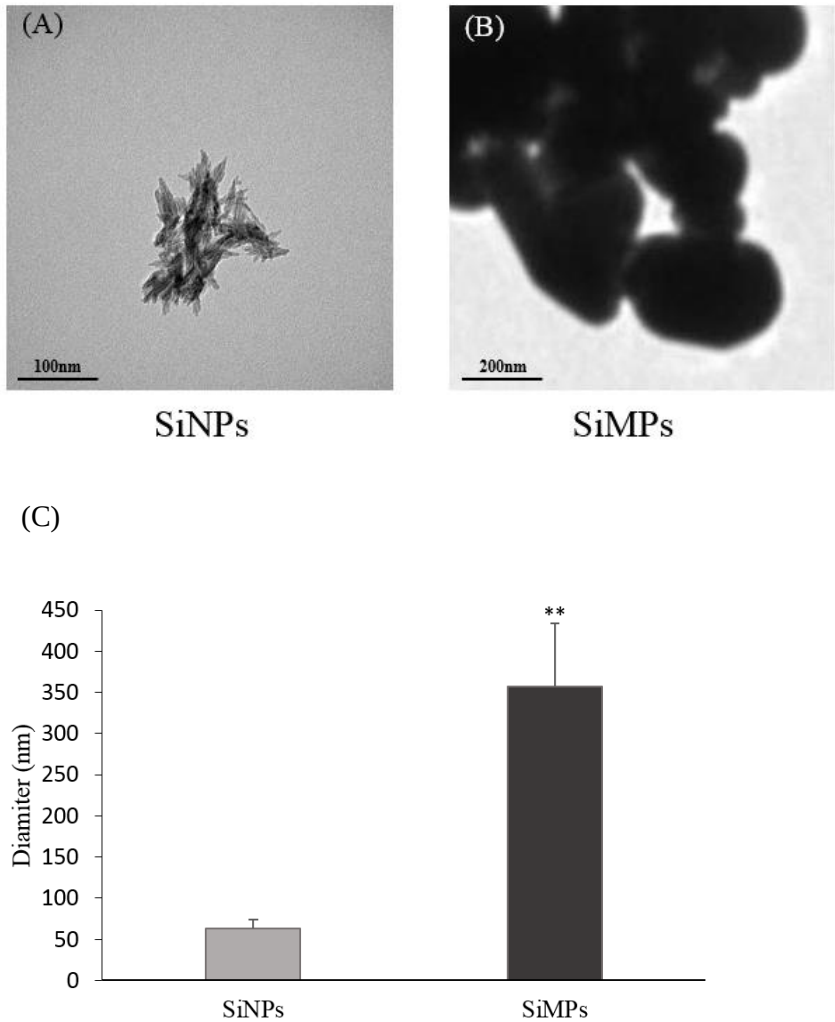

Figure 1. Morphology and size of SiNPs and SiMPs obtained by transmission electron microscopy (TEM).

TEM image of SiNPs (A) and SiMPs (B). Size distributions of SiNPs and SiMPs measured by TEM (C). Primary particles showed sizes of SiNPs and SiMPs were 62.79 ± 11.27nm and 357.20 ± 76.30nm, respectively. Asterisks indicate a statistically significant difference from SiNPs (*P<0.05, **P<0.01).

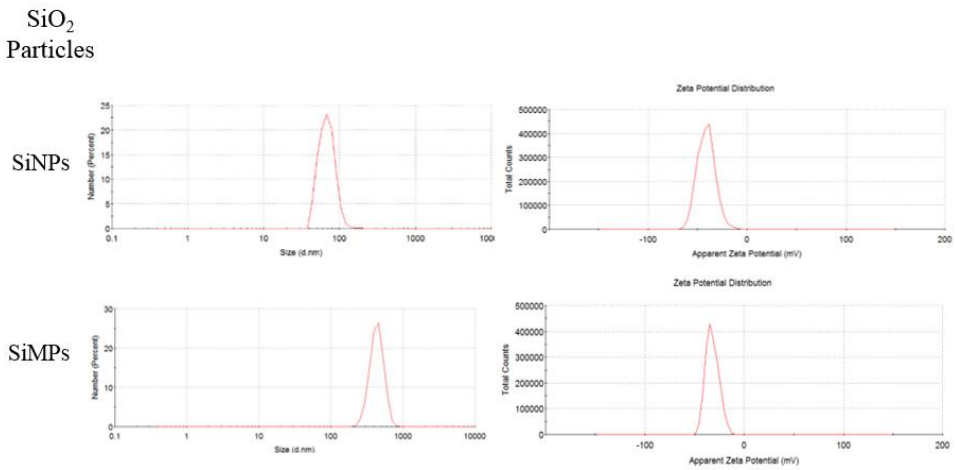

Figure 2. Hydrodynamic size and zeta potential values of SiNPs and SiMPs measured by dynamic light scattering (DLS) in water.

(A) DLS-analysis showed hydrodynamic size of SiNPs and SiMPs were 70.34 nm and 479.9nm.

(B) The zeta potential of SiNPs and SiMPs were -32.2mV and -41.2mV, respectively.

Table 1. Physico-chemical characterization of SiNPs

Particle Diameter (nm) [a]	Hydrodynamic size (nm) [b]	Zeta-potential (mV) [c]
62.79 ± 11.26	69.35	-32.2

[a] Diameter determined in deionized water by TEM

[b] Hydrodynimic size determined in deionized water by DLS

[c] Zeta-potential determined by DLS

Cytotoxicity assay of SiNPs

We conducted trypan blue exclusion assay to measure cytotoxicity. Different concentrations (0-5,000μg/ml) of SiNPs was treated. When 5,000μg/ml of SiNPs was treated, 70~80% cells viability was observed. Cell viability was 76.99% when 5,000μg/ml of SiNPs was treated (Fig. 3). The dose of SiNPs was determined as optimal dose for the following GJIC experiments to assess the highest levels of toxicity.

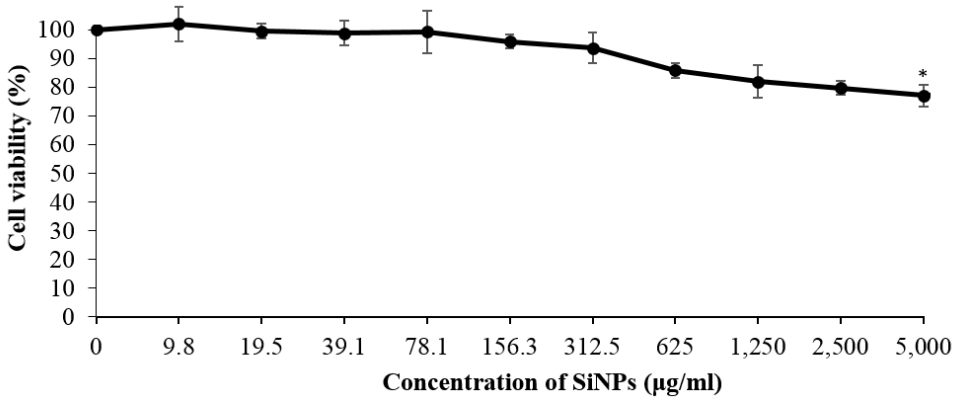

Figure 3. The effects of SiNPs on cell viability in WB-F344 cells.

When 5,000μg/ml of SiNPs was treated, 70~80% cells viability was observed. Cell viability was 76.99% when 5,000μg/ml of SiNPs was treated. All data were means ± S.D. of independent experiments performed in triplicate. Asterisks indicate a statistically significant difference from the control group (*P<0.05, **P<0.01).

SiNPs inhibited dye transfer time dependently in SL/DT assay

The function of GJIC was evaluated in a time course study using SL/DT method. SiNPs inhibited GJIC the most (by 37.75%) at 12 hours compared to normal control in 24 hours. The optimal time point was determined to be 12 hours for following dose dependent manner study of GJIC (Fig. 4).

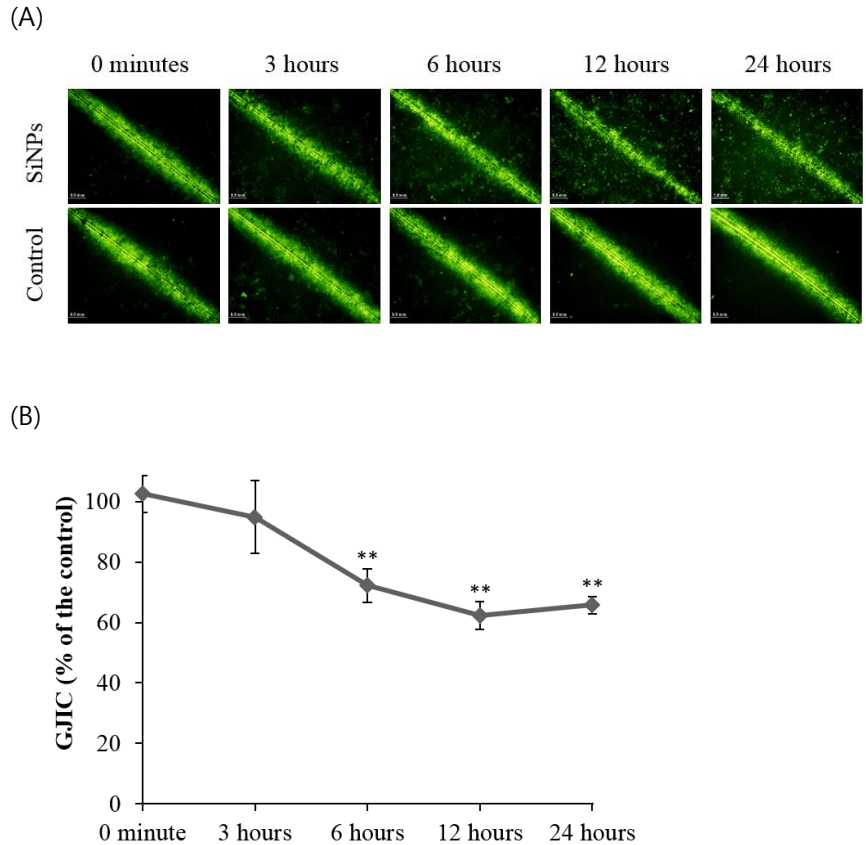

Figure 4. SiNPs inhibited dye transfer time dependently in WB-F344 cells in SL/DT assay.

(A) SL/DT assay after treatment with 5,000μg/ml SiNPs (Original magnification x100).

(B) Quantitative analysis of relative dye transfer.

SiNPs inhibited GJIC the most at 12 hours by 37.75% compared to normal control in 24 hours. All data were means ± S.D. of independent experiments performed in triplicate. Asterisks indicate a statistically significant difference from the control group (*P<0.05, **P<0.01).

SiNPs inhibited dye transfer dose dependently in SL/DT assay

According to the results of cytotoxicity, 5,000μg/ml, 1,000μg/ml and 200μg/ml of SiNPs was selected for dose dependent manner study of GJIC. SiNPs inhibited dye transfer in dose dependent manner by 38.57% at 5,000μg/ml and 25.35% at 1,000μg/ml by SiNPs (Fig. 5).

(A)

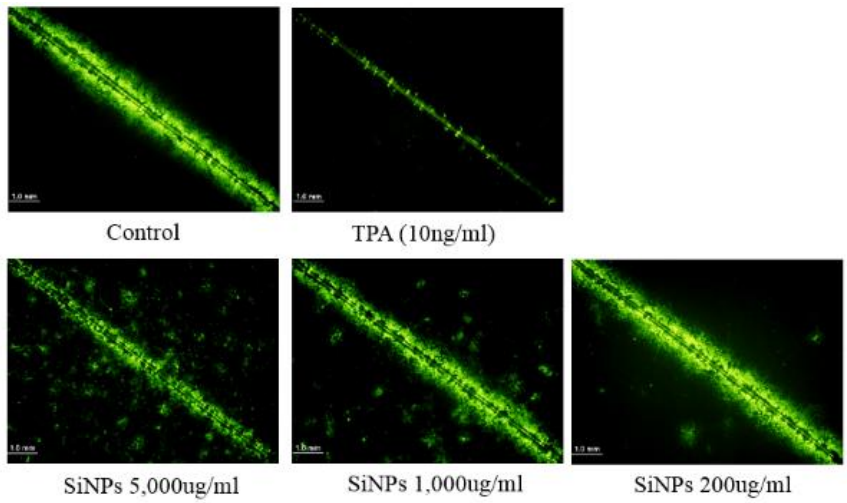

(B)

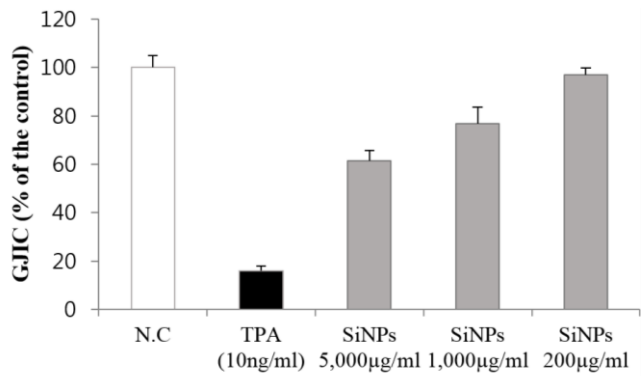

Figure 5. SiNPs inhibited dye transfer dose dependently in WB-F344 cells in SL/DT assay.

(A) SL/DT assay after treatment with SiNPs (original magnification x100).

(B) Quantitative analysis of relative dye transfer.

SiNPs inhibited dye transfer dose dependently by 38.57% at 5,000μg/ml, 25.35% at 1,000μg/ml by SiNPs. All data were means ± S.D. of independent experiments performed in triplicate. Asterisks indicate a statistically significant difference from the control group (*P<0.05, **P<0.01).

SiNPs inhibited expression of Cx43 dose dependently in immunofluorescence staining

Immunofluorescence staining was performed to determine expression level and localization of Cx43 protein. The expression of Cx43 decreased in dose dependent manner after treatment of SiNPs for 12 hours (Fig. 6). This result supported the results of SL/DT assay.

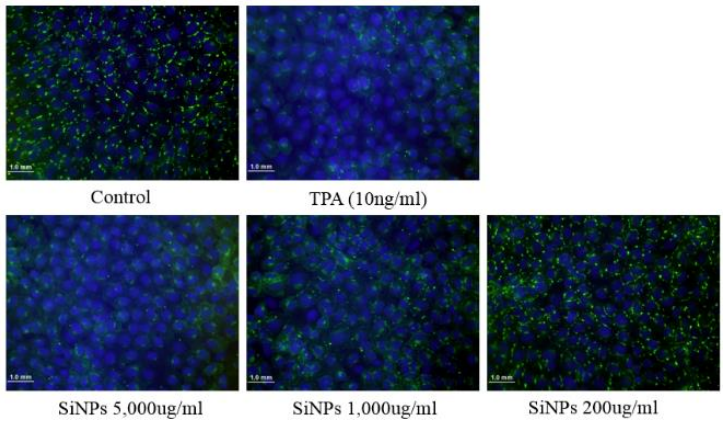

Figure 6. SiNPs inhibited expression of Cx43 dose dependently in WB-F344 cells in immunofluorescence staining.

Expression level and localization of Cx43 by immunofluorescence staining (Green). Nuclei was stained with DAPI (Blue) (Original magnification ×640). SiNPs decreased the expression of Cx43 after treatment in dose dependent manner for 12 hours.

SiNPs phosphorylated Cx43 dose dependently in western blot assay

Western blot analysis was performed to see how SiNPs inhibit GJIC in protein level. Three major bands (P0, P1 and P2) were detected on membrane at 39-44kDa with the Cx43 antibody, and mobility shifts from band P0 to P1 or P2 indicate the hyperphosphorylation of Cx43. In untreated cells, Cx43 was detected on only P0 and P1 band but cells exposed to SiNPs decreased the phosphorylation ratio (P2/P0) of Cx43 in dose dependent manner by 0.72 at 5,000μg/ml and 0.54 at 1,000μg/ml (Fig. 7A and 7B).

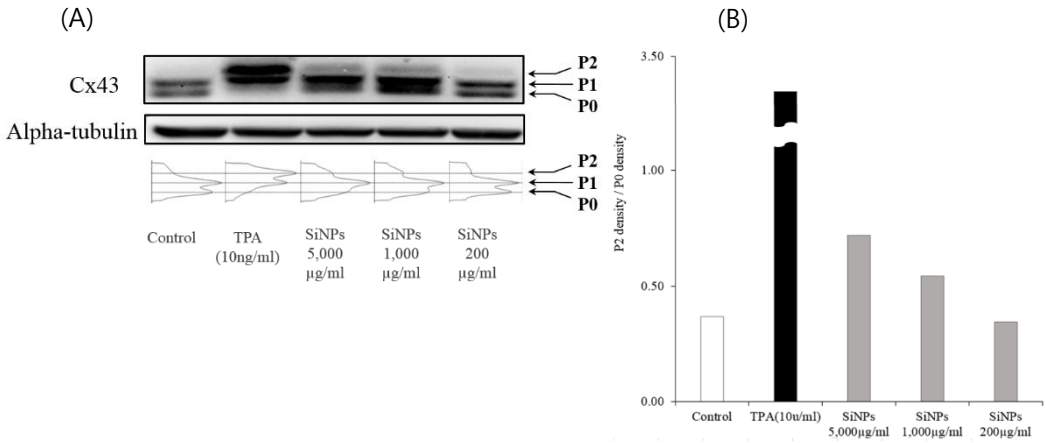

Figure 7. SiNPs phosphorylated Cx43 dose dependently in WB-F344 cells in western blot assay.

(A) Western blot assay of Cx43 after treatment with SiNPs.

(B) Quantitative analysis of P2 density/P0 density.

Phosphorylation ratio (P2/P0) of Cx43 decreased in dose dependent manner by 0.72 at 5,000μg/ml, 0.54 at 1,000μg/ml and 0.34 at 200μg/ml of SiNPs.

SiNPs activated MAPK pathway

Western blot analysis was performed to determine phosphorylation state of kinases including ERK1/2, MEK and PKC. SiNPs activated phosphorylation of ERK1/2 and MEK kinase in a dose dependent manner (Fig. 7A, 7B and 7C). Interestingly, SiNPs did not activated phosphorylation of PKC (Fig. 7A and 7D).

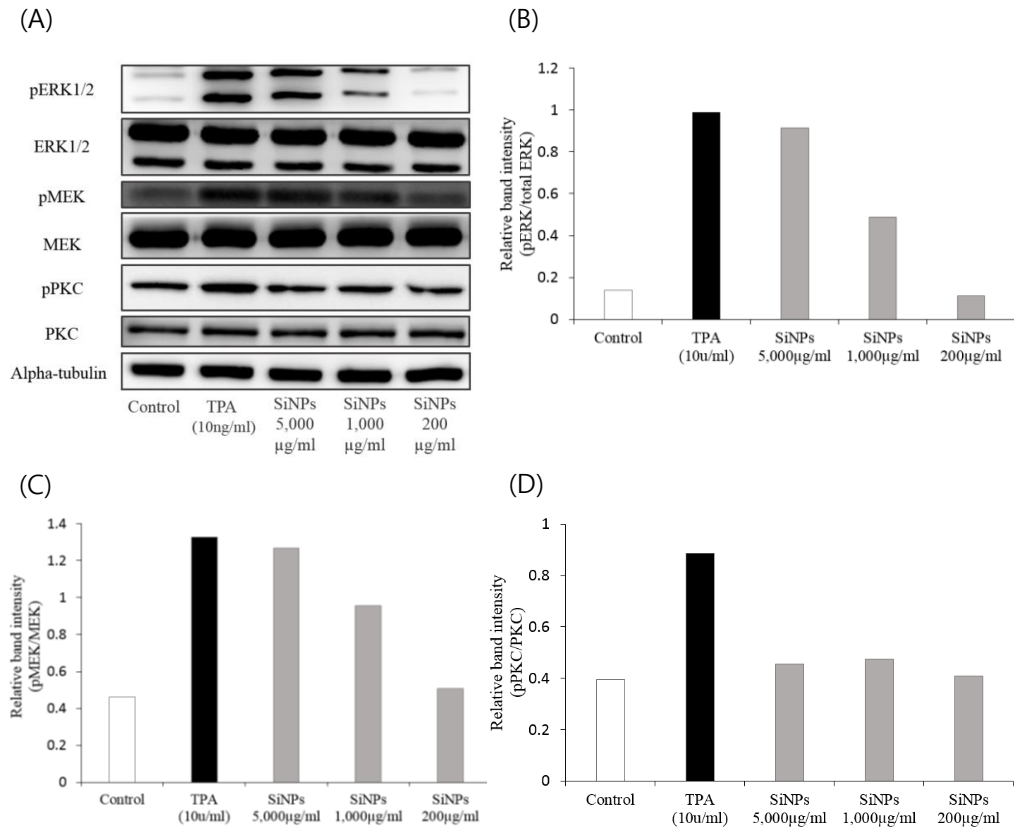

Figure 8. SiNPs activated MAPK pathway in WB-F344 cells.

(A) Western blot assay of kinases after treatment with SiNPs.

(B, C, D) Quantitative analysis of relative density.

EKR1/2 and MEK were phosphorylated in dose dependent after treatment of SiNPs. However, PKC was not phosphorylated by SiNPs.

SiNPs recovered inhibition of GJIC with MAPKs pathway inhibitors

We further determined the inhibition effect of ERK1/2 and MEK kinases on GJIC by using inhibitors. Inhibitions of dye transfer of lucifer yellow and expression of Cx43 induced by 5,000μg/ml of SiNPs for 12 hours was significantly recovered with pretreatment with ERK1/2 inhibitor and MEK inhibitor prior to treatment with SiNPs while PKC inhibitor did not recover SiNPs-induced inhibition of GJIC. Dye transfer was inhibited in cells threated with only 5,000μg/ml of SiNPs by 38.47% compared to normal control and pretreated with inhibitors of ERK1/2 and MEK were recovered up to 22.83% and 18.63% compared to normal control, respectively in SL/DT assay (Fig. 9A and 9B). Furthermore, result of immunofluorescence staining supported result of SL/DT assay. Decreased expression level of Cx43 by 5,000μg/ml of SiNPs was significantly recovered after pretreatment with ERK1/2 inhibitor and MEK inhibitor prior to treatment with SiNPs while PKC inhibitor did not recovered the decreased expression level of Cx43 in immunofluorescence staining (Fig. 9C). Phosphorylation of Cx43 induced by 5,000 μg/ml of SiNPs was significantly recovered with pretreatment with ERK1/2 inhibitor and MEK inhibitor prior to treatment with SiNPs. However, PKC inhibitor did not recovered phosphorylation of Cx43 (Fig. 9D and 9E).

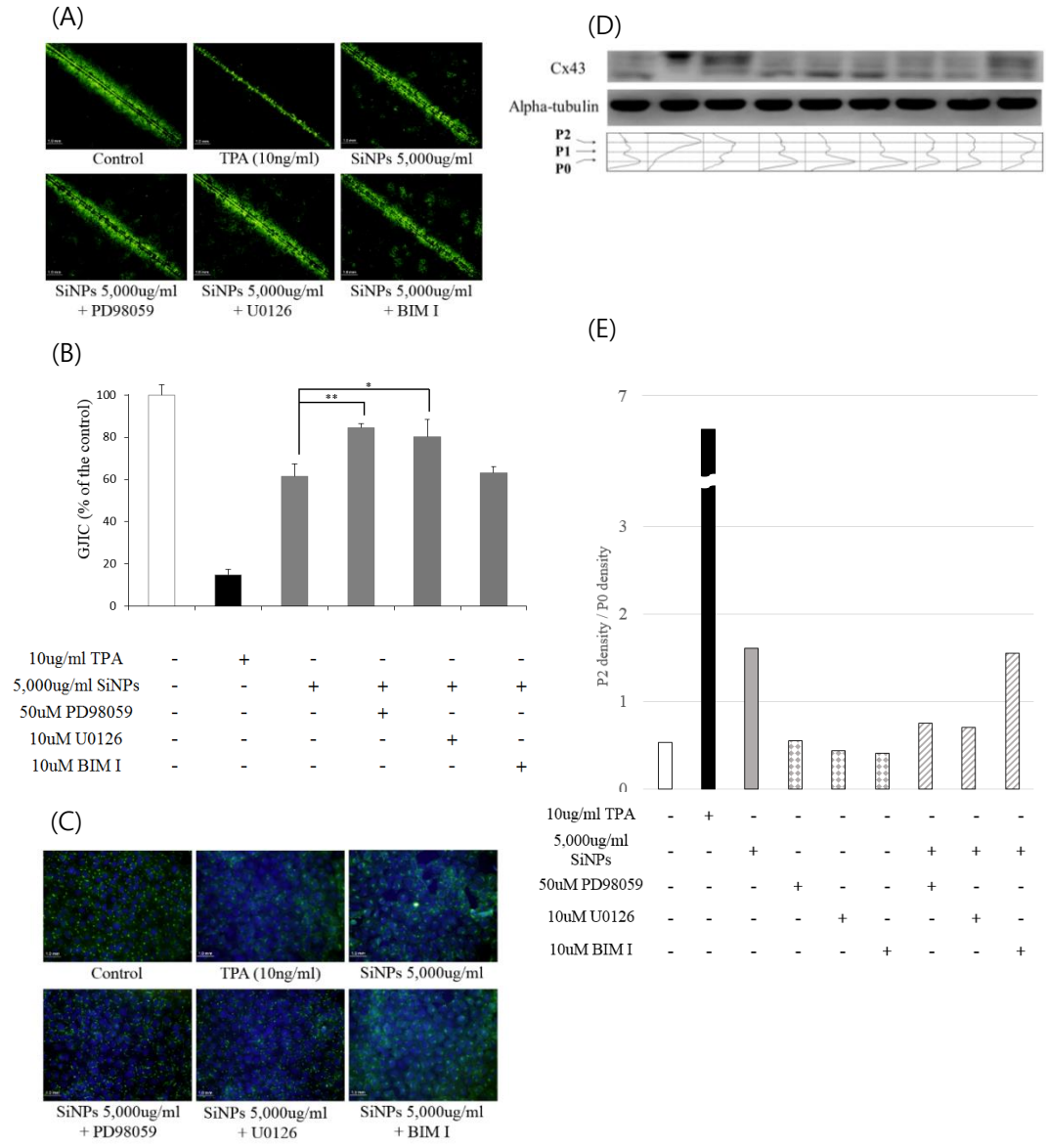

Figure 9. SiNPs recovered inhibition of GJIC with MAPKs pathway inhibitors in WB-F344 cells.

(A) SL/DT assay after treatment with 5,000 μg/ml SiNPs and inhibitors.

(Original magnification X100)

(B) Quantitative analysis of relative transfer.

(C) Immunofluorescence assay after treatment with 5,000 μg/ml SiNPs and inhibitors.

(Original magnification X640).

(D) Western blot assay after treatment with 5,000 μg/ml SiNPs and inhibitors.

(E) Quantitative analysis of P2 density / P0 density

(A, B) Dye transfer was inhibited in cells threated with only SiNPs by 38.47% compared to normal control and pretreated with inhibitors of ERK1/2 and MEK were recovered up to 22.83% and 18.63% compared to normal control, respectively in SL/DT assay. All data were means ± S.D. of independent experiments performed in triplicate. Asterisks indicate a statistically significant difference from the control group (*$P<0.05$, **$P<0.01$).

(C) Decreased expression level of Cx43 by 5,000μg/ml of SiNPs was recovered after pretreatment with ERK1/2 inhibitor and MEK inhibitor prior to treatment with SiNPs while PKC inhibitor did not recovered the decreased expression level of Cx43.

(D, E) Phosphorylation of Cx43 was recovered after pretreatment with ERK1/2 inhibitor and MEK inhibitor prior to treatment with SiNPs while PKC inhibitor did not recovered phosphorylation of Cx43.

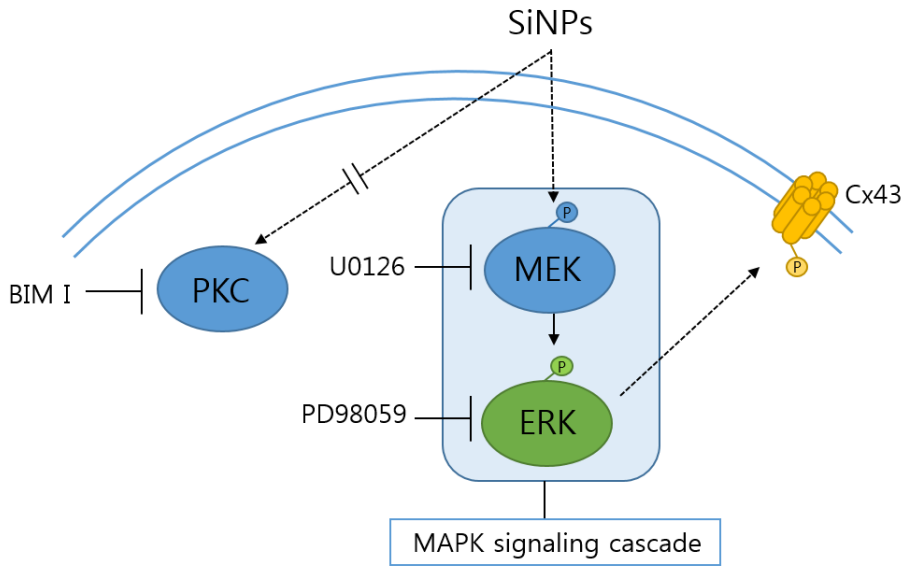

Figure 10. Schematic representation on the inhibition of GJIC by the SiNPs in WB-F344 cells.

Discussion

Nano-sized silica which is widely used in recent years should be investigated in diverse aspects including medical field due to different biocompatibility of nanoparticles from microparticles or bulk. Because amorphous silica is known to relative safe material in contrast to crystalline silica, it used in medical field [1, 4, 6, 9]. However, study about amorphous silica nanoparticle is still lack and a number of papers have recently been published on toxicity about amorphous silica nanoparticle [10, 11]. The aim of this study was to evaluate effect of amorphous silica about gap junctional intercellular communication.

Characterization of nanoparticles is a basic step to evaluate their potential toxicities because their toxicities have been revealed by many studies. Because a nanoparticle is defined as an object with at least one dimension of less than 100 nm, sizes of SiNPs can be verified to be below 100 nm by measuring them with TEM and DLS. In addition, TEM can characterize particles with respect to size and morphology and DLS can evaluate hydrodynamic size and zeta potential [15]. Shape of SiNPs was sharp and round-like. There was no impurity except for particles.

Experiment using agglomerated particle dispersions could result in misleading conclusions [42]. In the current study, SiNPs was not agglomerated based on results of TEM and DLS. First, sizes of SiNPs measured by DLS was slightly larger than hydrodynamic sizes measured by TEM. Hydrodynamic size is measured by adding particle diameter and electrical double layer by DLS. Agglomerative state can significantly increase the hydrodynamic size. Small gap of TEM-size and

hydrodynamic size indicate that SiNPs is not agglomerated. Thus, they are appropriate for nanotoxicity experiment. Second, zeta potential absolute value was more than 30 mV. The magnitude of absolute values of zeta-potential guarantees the stability of suspension. It has been reported that zeta potential absolute values of 30 mV or more are stable enough to overcome aggregation caused by the action of Van der Waals forces [43].

The ultra-small size property of nanomaterial makes it possible that nanomaterial may translocate biological barriers [44]. Nano-sized silica dioxide can be exposed via lots of routes and deposited in target organs [45].

We performed cytotoxicity test to determine optimal dose which would lead to 70~80% cell viability prior to GJIC study. Based on our results, 5,000 μg/ml of SiNPs was determined as optimal doses. Inhibition of GJIC is strongly involved in carcinogenesis because it causes failure of homeostasis which modulates cell proliferation and growth in multicellular organisms. SL/DT assay is the most frequently used assay for the assessment of GJIC because it is a simple functional assay for simultaneous assessment of GJIC [46]. Optimal dose of SiNPs determined by cytotoxicity test inhibited GJIC the most at 12 hours in a time course study by SL/DT assay. SiNPs inhibited dye transfer dose-dependently in SL/DT assay and expression of Cx43 dose-dependently in immunofluorescence staining. These results support our suggestion that SiNPs can inhibit.

We tried to investigate the cause of alteration in expression of Cx43 by western blot. It was generally attributed to two mechanisms. First, phosphorylation of Cx43 in the plasma membrane can induce alteration of assembly and stability in gap junctions [38]. Phosphorylation of connexin is associated with channel junctionality

and inhibition of GJIC. Second, production of main gap junction protein itself such as Cx43 can be decreased at mRNA level [47]. Numerous studies have shown that the phosphorylation state of connexin is affected by several exogenous chemicals such as 18alpha-glycyrrhetinic acid, 12-0-tetradecanoylphorbol-13-acetate, dieldrin, and heptachlor epoxide [34, 38]. At much higher dose of SiNPs, Cx43 was much more phosphorylated. If GJIC is inhibited at mRNA level, density of Cx43 will be decreased compared to loading control. The finding that SiNPs inhibited GJIC by phosphorylation of Cx43 was confirmed by western blot analysis.

To investigate the mechanism of inhibition of GJIC with SiNPs, we determined which kinase was phosphorylated by SiNPs using inhibitors prior to treatment with SiNPs. Activation of MAPK pathway has been reported to play a major role in the inhibition of gap junction by phosphorylation in response to various extracellular stimuli. The MAPK pathway is a chain of proteins in the cell that can communicate a signal from a receptor on the surface of cells. Serine/threonine-selective protein kinases (ERK) and serine/tyrosine/threonine kinase (MEK) can activate connexon, each of which is formed by six connexins by exposure to a substance in a series of kinases cascades. Once Src is activated, it in turn activates MAPK pathway and induces conformational change of connexin [38].

The inhibitory activity of SiNPs on GJIC was restored by ERK inhibitor and MEK inhibitor, but not by PKC inhibitor. This indicates a positive link between SiNPs-induced inhibitory effect of GJIC and MAPK pathway. Increased MEK and ERK phosphorylation has been reported in response to well-known several carcinogens such as TPA and DDT [48, 49].

We hypothesized that SiNPs induced inhibition of GJIC. SL/DT assay, immunofluorescence staining, and western blot analysis were performed to evlaluate effect of SiNPs to GJIC and to elucidate the related mechanism. Our results demonstrate that SiNPs can induce inhibition of GJIC time dependently and dose dependently. The inhibition of GJIC was involved to phosphorylation of Cx43 by MAPK pathway.

Further studies are needed based on this study. *In vivo* carcinogenicity test should be performed to clarify the carcinogenic effect of GJIC inhibition. Additionally, the mechanism study should be performed because MAPK mechanism can be realted to Ras/Raf pathway [50].

Considering the result of this study, we should consider the risk of SiNPs being exposed to humans. For example, in medical field, silica as cancer-targeted probe is exposed a concentration of about 0.1μg/ml in circulatory system [51]. According to this study, amorphous silica of 0.1μg/ml did not affect cytotoxicity and GJIC, so it may be safe to use an appropriated amount of amorphous silica. However, when injecting SiNPs into a high concentration, the effects on GJIC should be considered by referring to this study. As there are advantages and disadvantages of SiNPs, the benefit and risk should be considered carefully.

In conclusion, we consider that this is the first study to clarify the inhibition activity of GJIC with SINPs and its mechanism, and this study can provide the toxicological information about the potential risk of SiNPs.

References

1. Duncan, T.V., Applications of nanotechnology in food packaging and food safety: barrier materials, antimicrobials and sensors. J Colloid Interface Sci, 2011. 363(1): p. 1-24.
2. Rauch, J., W. Kolch, S. Laurent, and M. Mahmoudi, Big signals from small particles: regulation of cell signaling pathways by nanoparticles. Chem Rev, 2013. 113(5): p. 3391-406.
3. Nabeshi, H., T. Yoshikawa, K. Matsuyama, Y. Nakazato, K. Matsuo, A. Arimori, M. Isobe, S. Tochigi, S. Kondoh, T. Hirai, T. Akase, T. Yamashita, K. Yamashita, T. Yoshida, K. Nagano, Y. Abe, Y. Yoshioka, H. Kamada, T. Imazawa, N. Itoh, S. Nakagawa, T. Mayumi, S. Tsunoda, and Y. Tsutsumi, Systemic distribution, nuclear entry and cytotoxicity of amorphous nanosilica following topical application. Biomaterials, 2011. 32(11): p. 2713-24.
4. Uboldi, C., G. Giudetti, F. Broggi, D. Gilliland, J. Ponti, F.J.M.R.G.T. Rossi, and E. Mutagenesis, Amorphous silica nanoparticles do not induce cytotoxicity, cell transformation or genotoxicity in Balb/3T3 mouse fibroblasts. 2012. 745(1): p. 11-20.
5. Contado, C., Nanomaterials in consumer products: a challenging analytical problem. Front Chem, 2015. 3: p. 48.
6. Jaganathan, H. and B. Godin, Biocompatibility assessment of Si-based nano- and micro-particles. Adv Drug Deliv Rev, 2012. 64(15): p. 1800-19.

7. Gady, B., D.J. Quesnel, D.S. Rimai, S. Leone, and P. Alexandrovich, Effects of silica additive concentration on toner adhesion, cohesion, transfer, and image quality. Journal of Imaging Science and Technology, 1999. 43(3): p. 288-294.

8. Silica in the workplace. Industrial Accident Prevention Association, 2008.

9. Foldbjerg, R., J. Wang, C. Beer, K. Thorsen, D.S. Sutherland, and H. Autrup, Biological effects induced by BSA-stabilized silica nanoparticles in mammalian cell lines. Chem Biol Interact, 2013. 204(1): p. 28-38.

10. Ahamed, M., Silica nanoparticles-induced cytotoxicity, oxidative stress and apoptosis in cultured A431 and A549 cells. Hum Exp Toxicol, 2013. 32(2): p. 186-95.

11. Wiemann, M., U.G. Sauer, A. Vennemann, S. Bäcker, J.-G. Keller, L. Ma-Hock, W. Wohlleben, and R.J.N. Landsiedel, In Vitro and In Vivo Short-Term Pulmonary Toxicity of Differently Sized Colloidal Amorphous SiO2. 2018. 8(3): p. 160.

12. Ryu, H.J., N.-w. Seong, B.J. So, H.-s. Seo, J.-h. Kim, J.-S. Hong, M.-k. Park, M.-S. Kim, Y.-R. Kim, and K.-B.J.I.j.o.n. Cho, Evaluation of silica nanoparticle toxicity after topical exposure for 90 days. 2014. 9(Suppl 2): p. 127.

13. Farcal, L.R., C. Uboldi, D. Mehn, G. Giudetti, P. Nativo, J. Ponti, D. Gilliland, F. Rossi, and A. Bal-Price, Mechanisms of toxicity induced by SiO2 nanoparticles of in vitro human alveolar barrier: effects on cytokine production, oxidative stress induction, surfactant proteins A mRNA

expression and nanoparticles uptake. Nanotoxicology, 2013. 7(6): p. 1095-110.

14. Landsiedel, R., L. Ma-Hock, A. Kroll, D. Hahn, J. Schnekenburger, K. Wiench, and W. Wohlleben, Testing metal-oxide nanomaterials for human safety. Adv Mater, 2010. 22(24): p. 2601-27.

15. Hackenberg, S., A. Scherzed, A. Technau, M. Kessler, K. Froelich, C. Ginzkey, C. Koehler, M. Burghartz, R. Hagen, and N. Kleinsasser, Cytotoxic, genotoxic and pro-inflammatory effects of zinc oxide nanoparticles in human nasal mucosa cells in vitro. Toxicol In Vitro, 2011. 25(3): p. 657-63.

16. Magaye, R., J. Zhao, L. Bowman, and M. Ding, Genotoxicity and carcinogenicity of cobalt-, nickel- and copper-based nanoparticles. Exp Ther Med, 2012. 4(4): p. 551-561.

17. Warheit, D.B., T.R. Webb, C.M. Sayes, V.L. Colvin, and K.L.J.T.s. Reed, Pulmonary instillation studies with nanoscale TiO2 rods and dots in rats: toxicity is not dependent upon particle size and surface area. 2006. 91(1): p. 227-236.

18. Chang, J.-C., S.-h. Hsu, and H.-L.J.B. Su, The regulation of the gap junction of human mesenchymal stem cells through the internalization of quantum dots. 2009. 30(10): p. 1937-1946.

19. Chen, Y.-C., J.-K. Hsiao, H.-M. Liu, I.-Y. Lai, M. Yao, S.-C. Hsu, B.-S. Ko, Y.-C. Chen, C.-S. Yang, D.-M.J.T. Huang, and a. pharmacology, The inhibitory effect of superparamagnetic iron oxide nanoparticle

(Ferucarbotran) on osteogenic differentiation and its signaling mechanism in human mesenchymal stem cells. 2010. 245(2): p. 272-279.

20. Tao, Z., B.B. Toms, J. Goodisman, and T.J.C.r.i.t. Asefa, Mesoporosity and functional group dependent endocytosis and cytotoxicity of silica nanomaterials. 2009. 22(11): p. 1869-1880.

21. Arnoldussen, Y.J., K.H. Anmarkrud, V. Skaug, R.N. Apte, A. Haugen, S.J.J.o.c.c. Zienolddiny, and signaling, Effects of carbon nanotubes on intercellular communication and involvement of IL-1 genes. 2016. 10(2): p. 153-162.

22. Raghunathan, V.K., M. Devey, S. Hawkins, L. Hails, S.A. Davis, S. Mann, I.T. Chang, E. Ingham, A. Malhas, and D.J.J.B. Vaux, Influence of particle size and reactive oxygen species on cobalt chrome nanoparticle-mediated genotoxicity. 2013. 34(14): p. 3559-3570.

23. Kim, S., J.E. Choi, J. Choi, K.-H. Chung, K. Park, J. Yi, and D.-Y.J.T.i.v. Ryu, Oxidative stress-dependent toxicity of silver nanoparticles in human hepatoma cells. 2009. 23(6): p. 1076-1084.

24. Nimlamool, W., R.M. Andrews, and M.M. Falk, Connexin43 phosphorylation by PKC and MAPK signals VEGF-mediated gap junction internalization. Mol Biol Cell, 2015. 26(15): p. 2755-68.

25. Chang, J.C., S.H. Hsu, and H.L. Su, The regulation of the gap junction of human mesenchymal stem cells through the internalization of quantum dots. Biomaterials, 2009. 30(10): p. 1937-46.

26. Grek, C.L., G. Prasad, V. Viswanathan, D.G. Armstrong, R.G. Gourdie, G.S.J.W.R. Ghatnekar, and Regeneration, Topical administration of a

connexin43-based peptide augments healing of chronic neuropathic diabetic foot ulcers: A multicenter, randomized trial. 2015. 23(2): p. 203-212.

27. Fukunaga, I., A. Fujimoto, K. Hatakeyama, T. Aoki, A. Nishikawa, T. Noda, O. Minowa, N. Kurebayashi, K. Ikeda, and K.J.S.c.r. Kamiya, In Vitro Models of GJB2-Related Hearing Loss Recapitulate Ca2+ Transients via a Gap Junction Characteristic of Developing Cochlea. 2016. 7(6): p. 1023-1036.

28. Wu, D., J. Zhao, D. Wu, and J.J.I.j.o.m.m. Zhang, Ultraviolet A exposure induces reversible disruption of gap junction intercellular communication in lens epithelial cells. 2011. 28(2): p. 239-245.

29. Berger, A.C., J.J. Kelly, P. Lajoie, Q. Shao, and D.W.J.J.C.S. Laird, Mutations in Cx30 that are linked to skin disease and non-syndromic hearing loss exhibit several distinct cellular pathologies. 2014. 127(8): p. 1751-1764.

30. Lampe, P.D., A.F.J.T.i.j.o.b. Lau, and c. biology, The effects of connexin phosphorylation on gap junctional communication. 2004. 36(7): p. 1171-1186.

31. Evans, W.H. and P.E.J.M.m.b. Martin, Gap junctions: structure and function. 2002. 19(2): p. 121-136.

32. Trosko, J. and R.J.C.D.T. Ruch, Gap junctions as targets for cancer chemoprevention and chemotherapy. 2002. 3(6): p. 465-482.

33. Ruch, R.J., W.J. Bonney, K. Sigler, X. Guan, D. Matesic, L.D. Schafer, E. Dupont, and J.E.J.C. Trosko, Loss of gap junctions from DDT-treated rat liver epithelial cells. 1994. 15(2): p. 301-306.

34. Matesic, D.F., H.L. Rupp, W.J. Bonney, R.J. Ruch, and J.E. Trosko, Changes in gap-junction permeability, phosphorylation, and number mediated by phorbol ester and non-phorbol-ester tumor promoters in rat liver epithelial cells. Mol Carcinog, 1994. 10(4): p. 226-36.

35. El-Fouly, M.H., J.E. Trosko, and C.-C. Chang, Scrape-loading and dye transfer: a rapid and simple technique to study gap junctional intercellular communication. Experimental cell research, 1987. 168(2): p. 422-430.

36. Hofer, A., J.C. Sáez, C.C. Chang, J.E. Trosko, D.C. Spray, and R.J.J.o.N. Dermietzel, C-erbB2/neu transfection induces gap junctional communication incompetence in glial cells. 1996. 16(14): p. 4311-4321.

37. Lee, K.M., J.Y. Kwon, K.W. Lee, and H.J. Lee, Ascorbic acid 6-palmitate suppresses gap-junctional intercellular communication through phosphorylation of connexin 43 via activation of the MEK-ERK pathway. Mutat Res, 2009. 660(1-2): p. 51-6.

38. Guo, Y., C. Martinez-Williams, K.A. Gilbert, and D.E. Rannels, Inhibition of gap junction communication in alveolar epithelial cells by 18alpha-glycyrrhetinic acid. Am J Physiol, 1999. 276(6 Pt 1): p. L1018-26.

39. Steuer, A., A. Schmidt, P. Babica, and J. Kolb. Effects of Nanosecond Pulsed Electric Fields on Cell-Cell Communication in a Monolayer. in 1st World Congress on Electroporation and Pulsed Electric Fields in Biology, Medicine and Food & Environmental Technologies. 2016. Springer.

40. Strober, W., Trypan blue exclusion test of cell viability. Current protocols in immunology, 2001. Appendix 3: p. A3. B. 1-A3. B. 3.

41. Lee, D.E., N.J. Kang, K.M. Lee, B.K. Lee, J.H. Kim, K.W. Lee, and H.J. Lee, Cocoa polyphenols attenuate hydrogen peroxide-induced inhibition of gap-junction intercellular communication by blocking phosphorylation of connexin 43 via the MEK/ERK signaling pathway. J Nutr Biochem, 2010. 21(8): p. 680-6.

42. Jiang, J., G. Oberdörster, and P. Biswas, Characterization of size, surface charge, and agglomeration state of nanoparticle dispersions for toxicological studies. Journal of Nanoparticle Research, 2009. 11(1): p. 77-89.

43. Antonio Alves Júnior, J. and J. Baptista Baldo, The Behavior of Zeta Potential of Silica Suspensions. New Journal of Glass and Ceramics, 2014. 04(02): p. 29-37.

44. Konczol, M., S. Ebeling, E. Goldenberg, F. Treude, R. Gminski, R. Giere, B. Grobety, B. Rothen-Rutishauser, I. Merfort, and V. Mersch-Sundermann, Cytotoxicity and genotoxicity of size-fractionated iron oxide (magnetite) in A549 human lung epithelial cells: role of ROS, JNK, and NF-kappaB. Chem Res Toxicol, 2011. 24(9): p. 1460-75.

45. Huang, X., L. Li, T. Liu, N. Hao, H. Liu, D. Chen, and F. Tang, The shape effect of mesoporous silica nanoparticles on biodistribution, clearance, and biocompatibility in vivo. ACS nano, 2011. 5(7): p. 5390-5399.

46. Vinken, M. and S.R. Johnstone, Gap Junction Protocols. 2016: Springer.

47. Tacheau, C., J. Laboureau, A. Mauviel, and F. Verrecchia, TNF-alpha represses connexin43 expression in HaCat keratinocytes via activation of JNK signaling. J Cell Physiol, 2008. 216(2): p. 438-44.

48. Ueda, Y., S. Hirai, S. Osada, A. Suzuki, K. Mizuno, and S. Ohno, Protein kinase C activates the MEK-ERK pathway in a manner independent of Ras and dependent on Raf. J Biol Chem, 1996. 271(38): p. 23512-9.

49. Shen, K. and R.F. Novak, DDT stimulates c-erbB2, c-met, and STATS tyrosine phosphorylation, Grb2-Sos association, MAPK phosphorylation, and proliferation of human breast epithelial cells. Biochem Biophys Res Commun, 1997. 231(1): p. 17-21.

50. Santarpia, L., S.M. Lippman, and A.K.J.E.o.o.t.t. El-Naggar, Targeting the MAPK–RAS–RAF signaling pathway in cancer therapy. 2012. 16(1): p. 103-119.

51. Benezra, M., O. Penate-Medina, P.B. Zanzonico, D. Schaer, H. Ow, A. Burns, E. DeStanchina, V. Longo, E. Herz, and S.J.T.J.o.c.i. Iyer, Multimodal silica nanoparticles are effective cancer-targeted probes in a model of human melanoma. 2011. 121(7): p. 2768-2780.

국 문 초 록

무정형 실리카 나노물질의

Gap junction의 세포간 신호전달 억제 기전에 대한 연구

무정형 실리카 나노물질(Amorphous silica nanoparticles, SiNPs)은 많은 산업 분야에서 다양하게 사용되고 있다. 결정형 실리카 나노물질과 비교하여 SiNPs는 보다 안정적인 특성을 가지고 있기 때문에 식품첨가제, 화장품, 자동차 산업뿐만 아니라 약물/DNA 전달, 항암치료, 효소 고정화, 치과용 연마제와 같은 의학분야에도 사용되어 왔다. 그러나 나노물질의 독특한 물리적, 화학적인 특성이 체내에서 더 강한 독성을 유발할 수 있기 때문에 주의하여 사용되어야 하고, 최근 SiNPs의 독성에 대한 연구가 발표되고 있지만 아직 SiNPs의 발암성에 대한 연구는 부족하다. 본 연구는 WB-F344 rat liver epithelial cells에서 Gap junction의 세포간 신호전달(Gap junctional intercellular communication, GJIC)에 대한 실험을 통해 SiNPs의 발암성에 대한 영향을 평가하였다. SiNPs의 특성을 확인하기 위하여 투과 전자현미경(Transmission electron microscopy, TEM), 동적광산란법(Dynamic light scattering, DLS)으로 SiNPs의 크기를

측정하였다. SiNPs를 TEM으로 측정한 입자 지름은 각각 62.79±11.26nm 이었고, DLS로 측정한 유체역학적 크기(Hydrodynamic size)는 각각 69.35nm 이었다. 그리고 세포독성 실험을 하여 세포에 유의미한 독성이 없는 가장 높은 농도를 SiNPs 5,000μg/ml로 결정하였고 GJIC 실험에 이 농도를 처치하였다. GJIC 실험으로서 가장 먼저 시간의존적 SL/DT assay를 수행하였다. SiNPs는 처치 후 12시간째 37.75%만큼 GJIC를 가장 많이 억제하였다. 또한, SiNPs는 SL/DT assay, 면역형광 염색, 웨스턴 블롯 분석에서 용량 의존적으로 GJIC를 억제하였다. SiNPs는 ERK1/2와 MEK 활성효소를 용량의존적으로 인산화하였지만 PKC 활성효소는 인산화하지 않았다. 또한 ERK 1/2 inhibitor, MEK inhibitor를 전처치하였을 때 GJIC의 억제가 유의미하게 회복되었으나 PKC inhibitor의 전처치에 의해서는 회복되지 않았다. 결론적으로, 무정형 실리카 나노물질은 WB-F344 rat liver epithelial cells에서 MAPK pathway의 기전을 통해, GJIC를 억제한다고 판단된다. 무정형 실리카 나노물질은 현재 임상에서도 사용되고 있으므로 상대적으로 고농도의 무정형 실리카 나노물질이 GJIC를 억제한 본 연구를 참고하여 적정 용량을 임상적으로 사용하여야 한다.

주요어: 나노물질; 실리카; 간극연결의 세포간 신호전달; Cx43

학번: 2014-21159